

CMB and Molecules at High Redshift

F. Combes

*Observatoire de Paris, DEMIRM,
61 Av. de l'Observatoire, F-75 014 Paris, France*

Abstract. It becomes possible now to detect cold molecules at high redshift in the millimeter domain. Since the first discovery in 1992 by Brown and van den Bout of CO lines at $z = 2.28$ in a gravitationally lensed starburst galaxy, nearly ten objects are now known to possess large quantities of molecular gas beyond $z = 1$ and up to $z \sim 5$, through millimeter and sub-millimeter emission lines. Even more objects have been detected in their continuum dust emission, and a few galaxies through millimeter absorption lines in front of quasars at $z \leq 1$.

The continuum dust emission is the most easily detected: for a starburst dust at $T_d \sim 60$ K, the emission peaks around $60 \mu\text{m}$, and falls as λ^{-4} at longer wavelengths. In the mm domain, the emission is then stronger for the more redshifted objects. For the CO lines, the situation is less favorable, and the reported detections are helped by gravitational amplification. The increase of the CMB temperature T_{bg} with redshift helps the rotational line excitation (especially at high z), but not its detection.

Absorption in front of quasars is a more sensitive probe of cold gas at high redshift, able to detect individual clouds of a few solar masses (instead of $10^{10} M_\odot$ for emission). Taking advantage of the small size of the QSO, very high spatial resolution (of the order of milli-arcsec) can be achieved, and high spectral (30m/s) resolution, due to the heterodyne technique. The sampled column-densities range between $N(\text{H}_2) = 10^{20}$ et 10^{24} cm^{-2} . The high sensitivity allows to detect a multitude of molecular lines in a single object (HCO^+ , HNC , HCN , N_2H^+ , C^{18}O , CS , H_2CO , CN , CCH , H_2S etc....), and compare the chemistry with the local one, at $z = 0$. From the diffuse components, one can measure the cosmic black body temperature as a function of redshift. The high column densities component allow to observe important molecules not observable from the ground, like O_2 , H_2O and LiH for example.

All these preliminary studies carry a great hope for what will be observed with future millimeter instruments, and some perspectives are given.

I MILLIMETER CO EMISSION LINES AT HIGH REDSHIFT

This is a rapidly evolving domain, and at present, only 8 systems are published (cf Table 1). The search of CO lines at high z has been triggered by the detection of the CO(3-2) line in emission in the Faint IRAS source F10214+4724 at $z = 2.28$ by Brown & Vanden Bout (1991, 1992). At this time, it was a redshift 30 times larger than that of the most distant CO emission discovered in a galaxy. The H_2 mass derived was reaching $10^{13} h^{-2} M_\odot$, with the standard CO- H_2 conversion ratio, a huge mass although the FIR to CO luminosities was still compatible with that of other more nearby starbursts. Since then, the derived H_2 mass has been reduced by large factors, both with better data and realizing that the source is amplified through a gravitational lens by a large factor (Solomon et al 1992, 1997).

After the first discovery, many searches for other candidates took place, but they were harder than expected, and only a few, often gravitationally amplified, objects have been detected: the lensed Cloverleaf quasar H 1413+117 at $z = 2.558$ (Barvainis et al. 1994), the lensed radiogalaxy MG0414+0534 at $z = 2.639$ (Barvainis et al. 1998), the possibly magnified object BR1202-0725 at $z = 4.69$ (Ohta et al. 1996, Omont et al. 1996), the amplified submillimeter-selected hyperluminous galaxy SMM02399-0136 (Frayser et al. 1998), at $z = 2.808$, and the magnified BAL quasar APM08279+5255, at $z = 3.911$, where the gas temperature derived from the CO lines is $\sim 200\text{K}$, maybe excited by the quasar (Downes et al. 1998). Recently Scoville et al. (1997) reported the detection of the first non-lensed object at $z = 2.394$, the weak radio galaxy 53W002, and Guilloateau et al. (1997) the radio-quiet quasar BRI 1335-0417, at $z = 4.407$, which has no direct indication of lensing. If the non-amplification is confirmed, these objects would contain the largest molecular contents known ($8\text{-}10 \cdot 10^{10}$

M_{\odot} with a standard CO/H₂ conversion ratio, and even more if the metallicity is low). The derived molecular masses are so high that H₂ would constitute between 30 to 80% of the total dynamical mass (according to the unknown inclination), if the standard CO/H₂ conversion ratio was adopted. The application of this conversion ratio is however doubtful, and it is possible that the involved H₂ masses are 3-4 times lower (Solomon et al. 1997).

TABLE 1. CO data for high redshift objects

Source	z	CO line	S mJy	ΔV km/s	MH ₂ $10^{10} M_{\odot}$	Ref
F10214+4724	2.285	3-2	18	230	2*	1
53W002	2.394	3-2	3	540	7	2
H 1413+117	2.558	3-2	23	330	6	3
MG 0414+0534	2.639	3-2	4	580	5*	4
SMM 02399-0136	2.808	3-2	4	710	8*	5
APM 08279+5255	3.911	4-3	6	400	0.3*	6
BR 1335-0414	4.407	5-4	7	420	10	7
BR 1202-0725	4.690	5-4	8	320	10	8

* corrected for magnification, when estimated

Masses have been rescaled to $H_0 = 75 \text{ km/s/Mpc}$. When multiple images are resolved, the flux corresponds to their sum

(1) Solomon et al. (1992), Downes et al (1995); (2) Scoville et al. (1997); (3) Barvainis et al (1994); (4) Barvainis et al. (1998); (5) Frayer et al. (1998); (6) Downes et al. (1998); (7) Guilloteau et al. (1997); (8) Omont et al. (1996)

It is surprising that very few starburst galaxies have been detected in the CO lines at intermediate redshifts (between 0.3 and 2), although many have been observed (e.g Yun & Scoville 1998, Lo et al 1999). A possible explanation is the lower probability of magnification by lenses in this range (cf Figure 1).

II DUST EMISSION IN STAR-FORMING GALAXIES

Most of the previous sources, detected in the CO lines, had previously been detected in the dust continuum. At high redshift, it becomes easier to detect the dust emission, because of the large K-correction (e.g. Blain & Longair 1993): the emission is roughly varying as ν^4 with the frequency ν in the millimeter range, until the maximum around $60 \mu\text{m}$. At one mm, it is even easier to detect objects at $z = 5$ than $z = 1$. This has motivated deep searches in blank fields with sensitive instruments, since they should be dominated by high redshift objects, if they exist in sufficient numbers. Their detection will give information about the star-formation rate as a function of redshift, a debated question: the maximum of star-formation rate, found around $z = 2$ from optical studies (Madau et al 1996) could shift to higher z if dust is obscuring the higher-redshift objects. From recent infrared lines observations (Pettini et al 1998), it does not seem a serious problem, however.

The first search was made with the SCUBA bolometer on JCMT (Hawaii) towards a cluster of galaxies, thought to serve as a gravitational lens for high- z galaxies behind (Smail et al 1997). The amplification is in average a factor 2. A large number of sources were found, all at large redshifts ($z > 1$), extrapolated to 2000 sources per square degree (above 4 mJy), revealing a large positive evolution with redshift, i.e. an increase of starbursting galaxies. Searches toward the Hubble Deep Field-North (Hughes et al 1998), and towards the Lockman hole and SSA13 (Barger et al 1998), have also found a few sources, allowing to derive a similar density of sources: 800 per square degree, above 3 mJy at $850 \mu\text{m}$. This already can account for 50% of the cosmic infra-red background (CIRB), that has been estimated by Puget et al (1996) and Hauser et al (1998) from COBE data. The photometric redshifts of these sources range between 1 and 3. Their identification with optical objects might be uncertain (Richards 1998). However, Hughes et al (1998) claim that the star formation rate derived from the far-infrared might be in some cases 10 times higher than derived from the optical, due to the high extinction. If only some of the sources have a redshift higher than 4, it will flatten the Madau curve at high z .

Eales et al (1999) surveyed some of the CFRS fields at $850 \mu\text{m}$ with SCUBA and found also that the sources can account for a significant fraction of the CIRB background ($\sim 30\%$). Their interpretation in terms of the

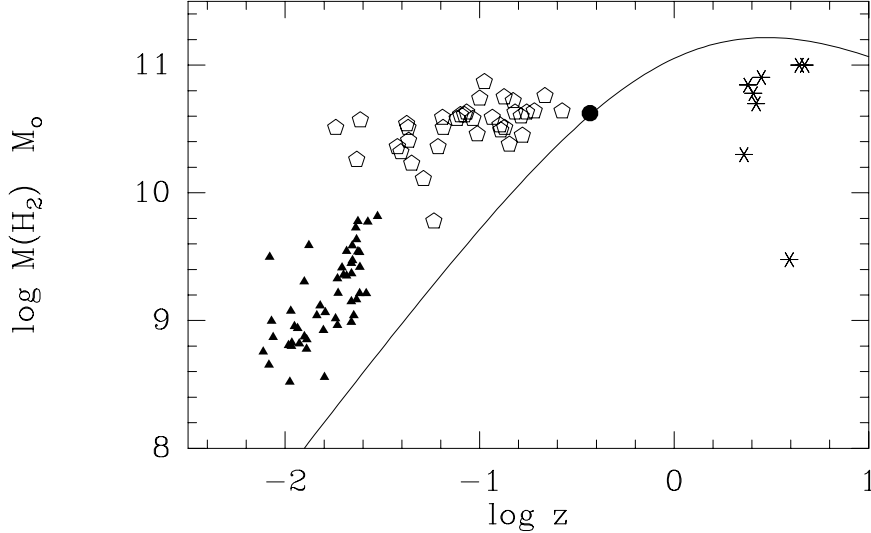


FIGURE 1. H_2 masses for the CO-detected objects at high redshift (filled stars), compared to the ultra-luminous-IR sample of Solomon et al (1997, open pentagons), and to the Coma supercluster sample from Casoli et al (1996, filled triangles). There is no detected object between 0.3 and 2.2 in redshift, except the quasar 3c48, marked as a filled dot (Scoville et al 1993, Wink et al 1997). The curve indicates the 3σ detection limit of $I(\text{CO}) = 1 \text{ K km/s}$ at the IRAM-30m telescope (equivalent to an rms of 1mK, with an assumed $\Delta V = 300 \text{ km/s}$). The points at high z can be detected well below this limit, since they are gravitationally amplified.

star formation history is however slightly different, in that they do not exclude that the submm luminosity density could evolve in the same way as the UV one. Deep galaxy surveys at 7 and $15\mu\text{m}$ with ISOCAM also see an evolution with redshift of star-forming galaxies: heavily extinguished starbursts represent less than 1% of all galaxies, but 18% of the star formation rate out to $z = 1$ (Flores et al 1999).

III MOLECULES IN ABSORPTION

Absorption techniques are also very efficient in the millimeter range, and a few systems have been discovered at high redshift, between $z = 0.2$ to 1 in the last years (Wiklind & Combes 1994, 95, 96; Combes & Wiklind 1996). The sensitivity is such that a molecular cloud on the line of sight of only a few solar masses is enough to detect a signal, while in emission, upper limits at the same distance are of the order of $10^{10} M_\odot$. Some general properties of the known absorbing systems are summarised in Table 2. They reveal to be the continuation at high column densities (10^{21} – 10^{24} cm^{-2}) of the whole spectrum of absorption systems, from the $\text{Ly}\alpha$ forest (10^{12} – 10^{19} cm^{-2}) to the damped $\text{Ly}\alpha$ and HI 21cm absorptions (10^{19} – 10^{21} cm^{-2}).

About 15 different molecules have been detected in absorption at high redshifts, in a total of 30 different transitions. This allows a detailed chemical study and comparison with local clouds (Wiklind & Combes 1997, Carilli et al 1998). Up to now, no significant variations in abundances have been found as a function of redshift, at least within the large intrinsic dispersion already existing within a given galaxy. Note that the high redshift allows us to detect some new molecular lines, never observed from the ground at $z = 0$, such as O_2 (Combes et al 1997), H_2O or LiH (Combes & Wiklind 1997, 1998). Molecular oxygen has not yet been detected in space, and water vapour appears to be extended and cold (see also the SWAS satellite preliminary results, Melnick et al 1999).

A The LiH molecule

Primordial molecules are thought to play a fundamental role in the early Universe, when stellar nucleosynthesis has not yet enriched the interstellar medium. After the decoupling of matter and radiation, the molecular

TABLE 2. Properties of molecular absorption line systems at high z

Source	z_a^a	z_e^b	N_{CO} cm^{-2}	N_{H_2} cm^{-2}	N_{HI} cm^{-2}	A_V^c	$N_{\text{HI}}/N_{\text{H}_2}$
PKS1413+357	0.24671	0.247	2.3×10^{16}	4.6×10^{20}	1.3×10^{21}	2.0	2.8
B3 1504+377A	0.67335	0.673	6.0×10^{16}	1.2×10^{21}	2.4×10^{21}	5.0	2.0
B3 1504+377B	0.67150	0.673	2.6×10^{16}	5.2×10^{20}	$< 7 \times 10^{20}$	< 2	< 1.4
B 0218+357	0.68466	0.94	2.0×10^{19}	4.0×10^{23}	4.0×10^{20}	850	1×10^{-3}
PKS1830–211A	0.88582	2.51	2.0×10^{18}	4.0×10^{22}	5.0×10^{20}	100	1×10^{-2}
PKS1830–211B	0.88489	2.51	1.0×10^{16d}	2.0×10^{20}	1.0×10^{21}	1.8	5.0
PKS1830–211C	0.19267	2.51	$< 6 \times 10^{15}$	$< 1 \times 10^{20}$	2.5×10^{20}	< 0.2	> 2.5

^aRedshift of absorption line ^bRedshift of background source ^cExtinction corrected for redshift using a Galactic extinction law ^dEstimated from the HCO^+ column density of $1.3 \times 10^{13} \text{ cm}^{-2}$ ^e21cm HI data taken from Carilli et al. 1992, 1993, 1998

radiative processes, and the formation of H_2 , HD and LiH contribute significantly to the thermal evolution of the medium (e.g. Puy et al 1993, Haiman, Rees & Loeb 1996). LiH has the lowest rotational first level (≈ 21 K above the ground level) and plays a unique role in the cooling of primordial clouds. Unfortunately, the first transition of HD is at very high frequency (2.7 THz), and the first LiH line, although only at 444 GHz, is not accessible from the ground at $z = 0$ due to H_2O atmospheric absorption.

Although the Li abundance is low (10^{-10} – 10^{-9}), the observation of the LiH molecule in the mm range is facilitated by its large dipole moment, $\mu = 5.9$ Debye. It has been proposed that the LiH molecules could smooth the primary CBR (Cosmic Background Radiation) anisotropies, due to resonant scattering, or create secondary anisotropies, and they could be the best way to detect primordial clouds as they turn-around from expansion (e.g. Maoli et al 1996). This motivated a search for LiH at very high redshifts ($z \sim 200$), which resulted in upper limits (de Bernardis et al 1993).

The predictions of the LiH abundance changed drastically in recent years, from the value of LiH/H_2 as high as $10^{-6.5}$ corresponding to a primordial LiH/H ratio of $\sim 10^{-12.5}$ (Lepp & Shull 1984), to the value of LiH/H of $< 10^{-15}$ in the postrecombination epoch, from Stancil et al. (1996). Indeed, quantum mechanical computations now predict the rate coefficient for LiH formation through radiative association to be 3 orders of magnitude smaller than previously thought from semi-classical methods (Dalgarno et al 1996). In more evolved dense clouds, when three-body association reactions and formation of dust grains are taken into account, a significant fraction of all lithium could turn into molecules. It is therefore important to try to detect LiH in a dense cloud, at high enough redshift that the line falls in an atmospheric window. This is the case for the absorbing cloud in the lensing galaxy in front of the B0218+357 quasar at a redshift of $z = 0.68466$. The H_2 column density is estimated to be $N(\text{H}_2) = 5 \times 10^{23} \text{ cm}^{-2}$ (Combes & Wiklind 1997). From a tentative detection (see figure 2) it was possible to deduce $\text{LiH}/\text{Li} \sim 1.5 \times 10^{-3}$. The uncertainty associated with the derived abundances are large, but the low LiH/Li ratio seems to exclude complete transformation of Li into LiH, as would be expected in very dense clouds (e.g. Stancil et al 1996, although the Li chemistry is not yet completely understood in dark clouds). However, it is likely that the cloud is clumpy, and in some of the more diffuse parts, LiH is photodissociated; some regions of the cloud could have a higher excitation temperature, in which case our computation under-estimates the LiH abundance.

B Determination of the Hubble constant

The best candidates to determine the Hubble constant via gravitational lenses, are quasars for which the multiple images are close together; then the lens can be only a bulge of a spiral galaxy, quite simple to model (contrary to widely separated images, where the lens is a cluster of galaxies). But then, the light rays pass close to the center of the lens galaxy, and absorption is likely to occur. Among the four absorption systems detected in the mm (cf Table 2), there are two cases of confirmed gravitational lenses, with two images (the two other cases are likely to be internal absorption). For these systems (B0218+357 and PKS1830-210), the separation between the two images is among the smallest recorded: 0.3 and 1 arcsec respectively. This makes

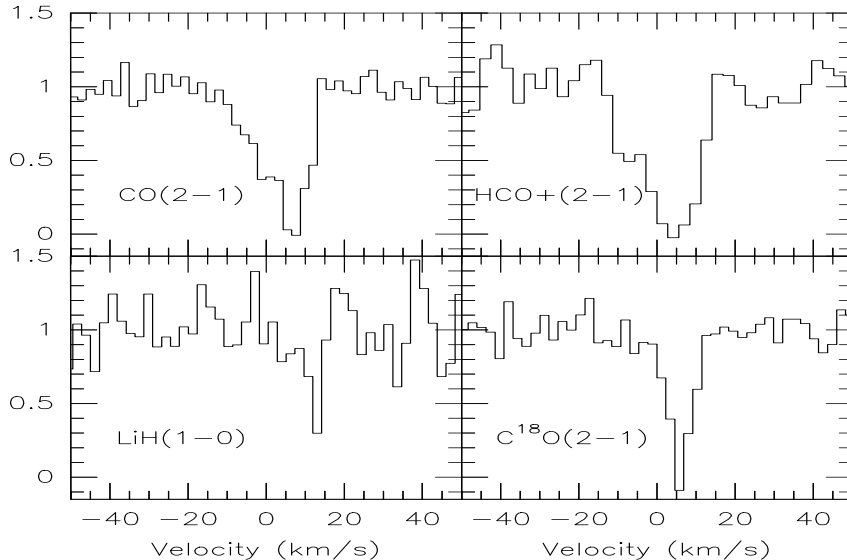


FIGURE 2. Tentative LiH detection towards B0218+357, at a redshift of $z = 0.68466$. The line is compared to optically thick lines like $\text{HCO}^+(2-1)$ and $\text{CO}(2-1)$, and more optically thin, such as $\text{C}^{18}\text{O}(2-1)$, normalised to the absorbed continuum.

these two objects good candidates for the determination of the Hubble constant, and the monitoring of the mm absorption can help to estimate the time-delay (Wiklind & Combes 1995, 1998). Already, Lovell et al (1998) determined a time delay of 26^{+4}_{-5} days in PKS1830-210 from radio-cm observations. Given the recently determined redshift of the quasar, of $z = 2.507$ (Lidman et al 1999, in prep), the derived Hubble constant is 65^{+16}_{-9} km/s/Mpc. In B0218+357, Biggs et al (1999, in press) were able to determine $H_0 = 69^{+7}_{-10}$ km/s/Mpc.

C Determination of CMB temperature

Molecular lines in the millimeter domain are a tool to determine the background temperature, not because molecular clouds are usually very cold, with a kinetic temperature of the order of 10-20K, but mainly because the lines are excited by collisions with H_2 . In diffuse regions, the collisional excitation is not enough, and the radiative excitation dominates. The excitation temperature of the molecules is then lower than the kinetic temperature, and close or equal to the background temperature T_{bg} . This is precisely the case of the gas absorbed in front of PKS1830-211, where $T_{ex} \sim T_{bg}$ for most of the molecules. The measurement of T_{ex} requires the detection of two nearby transitions. When the lower ones is optically thick, only an upper limit can be derived for T_{ex} . Ideally, the two transitions should be optically thin, but then the higher one is very weak, and long integration times are required.

The results obtained with the SEST-15m and IRAM-30m on different molecules agree and are plotted as a single point in figure 3. Surprisingly, the bulk of measurements points towards an excitation temperature lower than the background temperature at $z = 0.88582$, i.e. $T_{bg} = 5.20\text{K}$. We suspect that this could be due to a variation of the total continuum flux, due to a micro-lensing event.

IV PREDICTIONS AT EVEN HIGHER REDSHIFTS

At the present time, only objects at z below 10 have been detected. The amount of star formation at higher redshifts will be negligible for the global balance of the Universe, since the corresponding time is less than 3% of the Hubble time; however, it is of primordial importance to trace back the first stars formed, to understand star/galaxy formation processes just after recombination. Would it be possible, with the future millimetric instruments, that will gain at least a factor 20 in sensitivity with respect to the present ones, to detect starbursts at even higher redshifts?

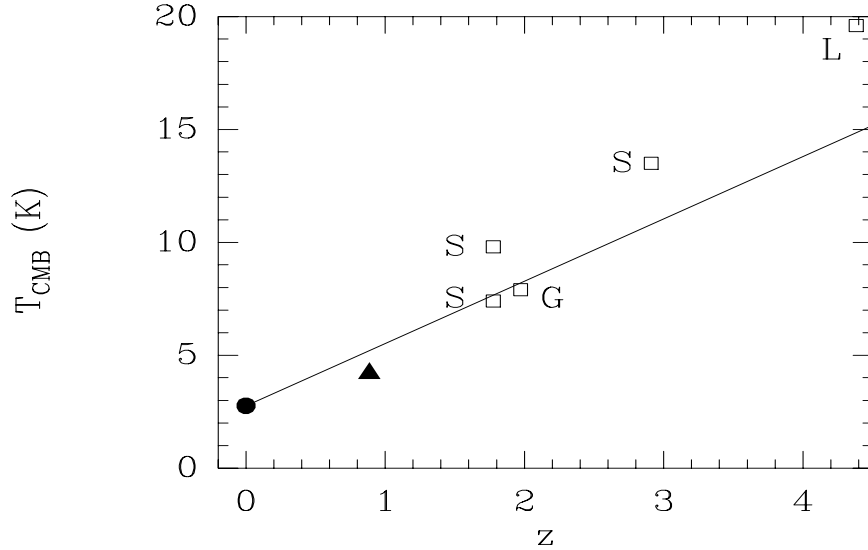


FIGURE 3. Summary of CMB temperature measurements as a function of redshift. The filled dot is from COBE (Mather et al 1994). The squares are upper limits obtained on the CI or CII from Songaila et al (1994ab, S), Lu et al (1996, L) and Ge et al (1997, G). Our point is the filled triangle. The line is the $(1+z)$ expected variation.

First, it will be easy to detect starbursts at $z \sim 5$ without the help of gravitational lensing as today (see figure 1). Beyond, since we do not know the nature of the objects, we can extrapolate their physical characteristics from the ultra-luminous FIR sample detected at lower z . As can be seen in Table 1, molecular masses range from 10^{10} to $10^{11} M_{\odot}$, the dust temperature is high, about 30-50K (up to 100K), and their size is strikingly small, below one kpc (300pc disks, Solomon et al 1997). In these conditions, the average column density of H_2 is 10^{24} cm^{-2} , and the dust becomes optically thick at $\lambda < 150 \mu\text{m}$. Two extreme simple models can be made about the corresponding molecular medium: either the gas is distributed in an homogeneous sphere, at a temperature of 50K, with a density of 10^3 cm^{-3} in average, or the gas is clumpy, distributed in cold dense clouds, with embedded hot cores. The expected flux coming from such starbursting regions in the various CO lines, and the continuum flux from the dust emission, can then be derived as a function of redshift (cf Combes et al 1999). The results of the two-component model, with kinetic temperatures 30 and 90 K at $z = 0$, and total gas mass $6 \cdot 10^{10} M_{\odot}$ is plotted in figure 4.

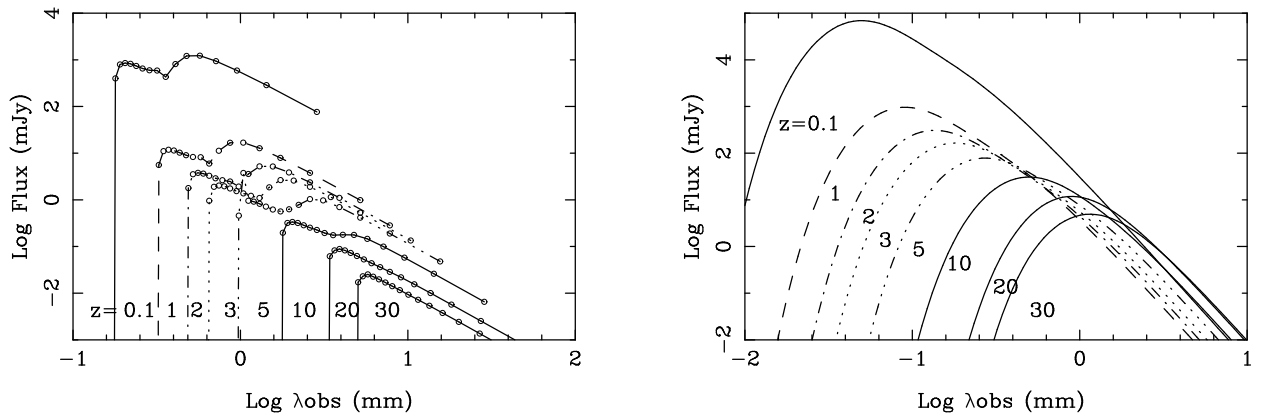


FIGURE 4. Expected flux for a starburst model in two-component clouds, of densities 10^4 and 10^6 cm^{-3} for various redshifts $z = 0.1, 1, 2, 3, 5, 10, 20, 30$, and $q_0 = 0.5$. Left are the CO lines, materialised each by a circle. Right is the continuum emission from dust.

This picture shows that, since the low- J CO lines are optically thick, their flux varies with the wavelength as λ^{-2} at large λ in the millimeter range. This means that the CO-lines detection will be less favoured at high redshift than the continuum emission. Unfortunately, the increase of the CMB temperature T_{bg} with redshift has not a significant effect on the detectability at high z : if the excitation temperature of the gas is indeed increased, the background emission to subtract is also increased in the same proportions. It is already much more difficult to detect objects at $z = 5$ than at $z = 1$, contrary to the dust emission. This conclusion is opposite to what was found by Silk & Spaans (1997) in their model. The most favourable wavelengths to detect the CO lines are always longer than 1mm (assuming that the kinetic temperature of the gas is the same as the dust temperature). We can note that it is already possible to detect now in the continuum such huge starbursts at any redshifts (up to 30). With the upcoming future millimeter instruments, it will be possible to detect them also in the CO lines, or detect much more modest starbursts in the continuum.

REFERENCES

1. Barger A.J., Cowie L.L., Sanders D.B. et al.: 1998, *Nature* 394, 248
2. Barvainis R., Alloin D., Guilloteau S., Antonucci R.: 1998, *ApJ* 492, L13
3. Barvainis R., Tacconi L., Antonucci R., Coleman P.: 1994, *Nature* 371, 586
4. Blain A.W., Longair M.S.: 1993, *MNRAS* 264, 509
5. Brown R., Vanden Bout P.: 1992, *ApJ* 397, L19
6. Brown R., Vanden Bout P.: 1991, *AJ* 102, 1956
7. Carilli C.L., Perlman E.S., Stocke J.T.: 1992, *ApJ* 400, L13
8. Carilli, C.L., Rupen, M.P., Yanny, B.: 1993, *ApJ* 412, L59
9. Carilli, C.L., Menten K.M., Reid M.J., Rupen, M.P., Yun M.S.: 1998, *ApJ* 494, 175
10. Carilli, C.L., Menten K.M., Reid M.J., Rupen, M.P., Claussen M.: 1998, in "Structure and Evolution of the Intergalactic Medium from QSO Absorption Line Systems", ed. P. Petitjean and S. Charlot, Editions Frontières, p. 325
11. Casoli F., Dickey J., Kazes I. et al.: 1996, *A&AS* 116, 193
12. Combes F., Wiklind T., Nakai N.: 1997, *A&A* 327, L17
13. Combes F., Wiklind T.: 1996, in "Cold gas at high redshift", ed. Bremer M., Rottgering H., van der Werf P., Carilli C.L. (Dordrecht:Kluwer), p. 215
14. Combes F., Wiklind T.: 1997, *ApJ* 486, L79
15. Combes F., Wiklind T.: 1998, *A&A* 334, L81
16. Combes F., Maoli R., Omont M.: 1999, *A&A* in press
17. Dalgarno A., Kirby K., Stancil P.C.: 1996, *ApJ* 458, 397
18. de Bernardis P., Dubrovich V., Encrenaz P. et al.: 1993, *A&A* 269, 1
19. Downes D., Neri R., Wiklind T., Wilner D.J., Shaver P.: 1998, *ApJ* preprint (astro-ph/9810111)
20. Downes D., Solomon P.M., Radford S.J.E.: 1995, *ApJ* 453, L65
21. Eales S.A., Lilly S.J., Gear W.K., Dunne L., Bond J.R., Hammer F., Le Fevre O., Crampton D.: 1999, *ApJL* in press (astro-ph/9808040)
22. Flores H., Hammer F., Thuan X. et al. : 1999, *ApJ* in press (astro-ph/9811202)
23. Frayer D.T., Ivison R.J., Scoville N.Z., et al., 1998, *ApJ* 506, L7
24. Ge J., Bechtold J., Black J.: 1997, *ApJ* 474, 67
25. Guilloteau S., Omont A., McMahon R.G., Cox P., PetitJean P.: 1997, *A&A* 328, L1
26. Haiman Z., Rees M.J., Loeb A.: 1996, *ApJ* 467, 522
27. Hauser M.G., Arendt R.G., Kelsall T., et al.: 1998, *ApJ* 508, 25
28. Hughes D.H., Serjeant S., Dunlop J. et al.: 1998, *Nature* 394, 241
29. Lepp S., Shull J.M.: 1984, *ApJ* 280, 465
30. Lo K.Y., Chen H-W., Ho P.T.P.: 1999, *A&A* 341, 348
31. Lovell J.E., Jauncey D.L., Reynolds J.E. et al.: 1998, *ApJ* 508, L51
32. Lu, L., Sargent, W. L. W., Womble, D. S., Barlow, T. A.: 1996, *ApJ*, 457, L1
33. Madau P., Ferguson H.C., Dickinson M.E. et al.: 1996, *MNRAS* 283, 1388
34. Maoli R., Ferruci V., Melchiorri F. et al: 1996, *ApJ* 457, 1
35. Mather, J. C., et al.: 1994, *ApJ*, 420, 439
36. Melnick G.J. et al.: 1999, *BAAS* 193, 7201
37. Ohta K., Yamada T., Nakanishi K., Kohno K., Akiyama M., Kawabe R.: 1996, *Nature* 382, 426
38. Omont A., Petitjean P., Guilloteau S., McMahon R.G., Solomon P.M.: 1996, *Nature* 382, 428
39. Pettini M., Kellog M., Steidel C.C. et al.: 1998, *ApJ* 508, 539

40. Puget J.L., Abergel A., Bernard J-P. et al. : 1996, A&A 308, L5
41. Puy D., Alecian G., Le Bourlot J., Léorat J., Pineau des Forêts G., 1993, A&A 267, 337
42. Richards E.R.: 1998, ApJ in press (astro-ph/9811098)
43. Scoville N.Z., Padin S., Sanders D.J. et al. : 1993, ApJ 415, L75
44. Scoville N.Z., Yun M.S., Windhorst R.A., Keel W.C., Armus L.: 1997, ApJ 485, L21
45. Silk J., Spaans M.: 1997, ApJ 488, L79
46. Smail I., Ivison R.J., Blain A.W.: 1997, ApJL 490, L5
47. Solomon P.M., Downes D., Radford S.J.E., Barrett J.W.: 1997, ApJ 478, 144
48. Solomon P.M., Downes D., Radford S.J.E.: 1992, Nature 356, 318
49. Songaila, A., Cowie L.L., Hogan C., Rugers M.: 1994a: Nature, 368, 599
50. Songaila, A., Cowie L.L., Vogt S. et al.: 1994b: Nature, 371, 43
51. Stancil P.C., Lepp S., Dalgarno A.: 1996, ApJ 458, 401
52. Yun M.S., Scoville N.Z.: 1998, ApJ 507, 774
53. Wiklind T., Combes F.: 1994, A&A 286, L9
54. Wiklind T., Combes F.: 1995, A&A 299, 382
55. Wiklind T., Combes F.: 1996, Nature 379, 139
56. Wiklind T., Combes F.: 1997, A&A 328, 48
57. Wiklind T., Combes F.: 1998, ApJ 500, 129
58. Wink J.E., Guilloteau S., Wilson T.L.: 1997, A&A 322, 427